AIP Journal of Applied Physics

Temperature-dependent failure mechanism of SnAg solder joints with Cu metallization after current stressing: Experimentation and analysis

C. K. Lin, Wei An Tsao, Y. C. Liang, and Chih Chen

Citation: Journal of Applied Physics **114**, 113711 (2013); doi: 10.1063/1.4821427
View online: http://dx.doi.org/10.1063/1.4821427
View Table of Contents: http://scitation.aip.org/content/aip/journal/jap/114/11?ver=pdfcov
Published by the AIP Publishing

Articles you may be interested in
The failure models of Sn-based solder joints under coupling effects of electromigration and thermal cycling
J. Appl. Phys. **113**, 044904 (2013); 10.1063/1.4789023

Effect of contact metallization on electromigration reliability of Pb-free solder joints
J. Appl. Phys. **99**, 094906 (2006); 10.1063/1.2193037

Electromigration failure mechanisms for SnAg 3.5 solder bumps on Ti Cr - Cu Cu and Ni (P) Au metallization pads
J. Appl. Phys. **96**, 4518 (2004); 10.1063/1.1788837

Mechanism of electromigration-induced failure in the 97Pb–3Sn and 37Pb–63Sn composite solder joints
J. Appl. Phys. **94**, 7560 (2003); 10.1063/1.1628388

Mean-time-to-failure study of flip chip solder joints on Cu/Ni(V)/Al thin-film under-bump-metallization
J. Appl. Phys. **94**, 5665 (2003); 10.1063/1.1616993

Re-register for Table of Content Alerts
Create a profile.
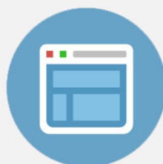
Sign up today!

[This article is copyrighted as indicated in the article. Reuse of AIP content is subject to the terms at: http://scitation.aip.org/termsconditions. Downloaded to] IP: 140.113.38.11 On: Wed, 30 Apr 2014 08:48:10

JOURNAL OF APPLIED PHYSICS **114**, 113711 (2013)

Temperature-dependent failure mechanism of SnAg solder joints with Cu metallization after current stressing: Experimentation and analysis

C. K. Lin, Wei An Tsao, Y. C. Liang, and Chih Chen[a)]
Department of Materials Science and Engineering, National Chiao Tung University, Hsin-chu 30010, Taiwan

(Received 8 May 2013; accepted 2 September 2013; published online 19 September 2013)

Temperature-dependent electromigration failure was investigated in solder joints with Cu metallization at 126 °C, 136 °C, 158 °C, 172 °C, and 185 °C. At 126 °C and 136 °C, voids formed at the interface of Cu_6Sn_5 intermetallic compounds and the solder layer. However, at temperature 158 °C and above, extensive Cu dissolution and thickening of Cu_6Sn_5 occurred, and few voids were observed. We proposed a model considering the flux divergency at the interface. At temperatures below 131 °C, the electromigration flux leaving the interface is larger than the in-coming flux. Yet, the in-coming Cu electromigration flux surpasses the out-going flux at temperatures above 131 °C. This model successfully explains the experimental results. © *2013 AIP Publishing LLC*. [http://dx.doi.org/10.1063/1.4821427]

I. INTRODUCTION

As microelectronic devices continue to produce high operation speeds and superior performance, the current density in interconnects continues to increase, and electromigration remains a critical reliability issue for interconnects.[1,2] Solder joints have been employed for interconnects in high-performance devices.[3–5] The diameter range of a solder bump is currently 70–100 μm. The diameter for a microbump has reduced dramatically to 20 μm in 3-dimensional integrated circuits (3D IC).[6–8] The cross-sectional area of a microbump is only 0.05 times the cross-sectional area of a flip-chip joint. Therefore, electromigration continues to be an important reliability issue for solder joints.[9–15]

Ni and Cu are the most popular under-bump metallization (UBM) materials. Cu exhibits superior wettability and a high reaction rate with solders.[16] During current stressing, electron flow enhances the dissolution of Cu into solders, causing a rapid consumption of Cu and a significant formation of Kirkendall voids.[17–20] Conversely, Ni exhibits a slow reaction rate with solders.[21–23] Therefore, solder joints with Ni UBMs possess larger electromigration lifetimes.[24–26] Electromigration in solder joints with Cu UBMs has been examined extensively.[17–20] Two major failure mechanisms have been identified: void formation[1,14,27] and the dissolution of intermetallic compounds (IMCs).[28–30] Recently, Ke *et al*. reported that void formation dominated the electromigration failure mechanism at high temperatures whereas the dissolution of IMCs for solder joints with Cu UBMs occurred at low temperatures.[31] In this study, we observed the reverse trend: the formation of voids at low temperatures and the dissolution of IMCs at high temperatures in the Cu-Sn system.

In this study, we investigated the electromigration failure mechanism for SnAg solder joints with 20 μm Cu metallization on the substrate side. Void formation dominated the electromigration failure mechanism at low stressing temperatures whereas the dissolution of Cu UBM occurred at high stressing temperatures. We also proposed a model that considers the Cu electromigration fluxes in Cu_6Sn_5 and the Cu electromigration fluxes in solder. The model successfully explains the experimental results.

[a)]Author to whom correspondence should be addressed. Electronic mail: chih@mail.nctu.edu.tw.

II. EXPERIMENTAL

Typical flip-chip solder joints were adopted for the electromigration tests. Fig. 1(a) shows the schematic drawing for the solder joints. On the chip side, 0.1 μm Ti was sputtered as an adhesion layer. Then 0.5 μm Cu was sputtered as a seed layer for the subsequent electroplating of Ni layer. A 2.0 μm layer of Ni was electroplated as the UBM. The metallization on the substrate side is 20-μm-thick Cu. The composition of solder is SnAg (2.6 wt. %). The diameter of UBM and passivation opening is 110 μm and 90 μm, respectively. The contact opening on the substrate side is 110 μm. The Al trace on the chip side is 65 μm wide and 1.5 μm thick whereas the Cu trace on the substrate side is 100 μm wide and 20 μm thick. Pre-solder of Sn-3.0Ag-0.5Cu was used on the substrate side when joining the flip-chip joints.

Four-point probes were used to monitor the resistance change during electromigration tests. Fig. 1(b) presents the schematic structure for the test layout. Currents were applied throng Nodes N2 and N3. Voltage was measured by Nodes N1 and N4. Only bump B2 and B3 were stressed by 1.3 A of current. The resistance measured included the bumps B2 and B3, as well as the Al trace connecting the bumps B2 and B3. The solder joints were stressed by 1.3 A at various temperatures, including 100 °C, 110 °C, 130 °C, 140 °C, and 150 °C. The calculated current density is 1.4×10^4 A/cm^2 based on the UBM opening. As the measured resistance increased 10 mΩ, the current stressing was terminated, and the electromigration failure mode was examined by a scanning electron microscope (SEM). Compositional analysis was performed by energy dispersive spectrometer (EDS).

III. RESULTS

The microstructure of the fabricated bump was shown in Fig. 2. Ternary IMCs of $(Cu,Ni)_6Sn_5$ formed in the interface

 © 2013 AIP Publishing LLC

[This article is copyrighted as indicated in the article. Reuse of AIP content is subject to the terms at: http://scitation.aip.org/termsconditions. Downloaded to] IP: 140.113.38.11 On: Wed, 30 Apr 2014 08:48:10

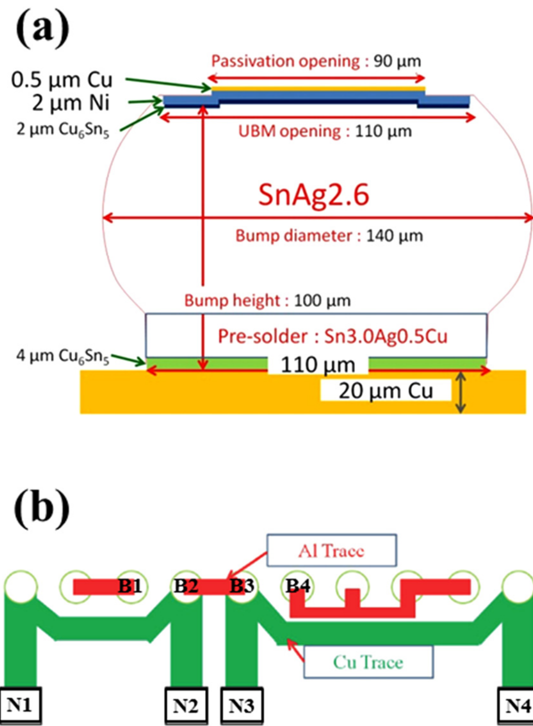

FIG. 1. (a) Schematic structure of the solder joint configuration used in this study. (b) Layouts for electromigration tests and Four-point structure for measuring bump resistance.

of Ni and solder on the chip side. The Cu on the chip side came from the substrate side.[32,33] On the substrate side, binary Cu_6Sn_5 IMCs formed at the interface of Cu metallization and the solder. The real temperature in solder joints may be higher than the ambient temperature during current stressing due to serious Joule heating effect in the stressing circuit.[34,35] Therefore, the real temperature needs to be calibrated. In this study, we employed the temperature coefficient of resistivity (TCR) to measure the real temperature in solder joints. The solder joint was placed in an oven, and we measured the resistance using the four point method as a function of the oven temperature. The real temperatures in solder joints during various stressing condition are listed in

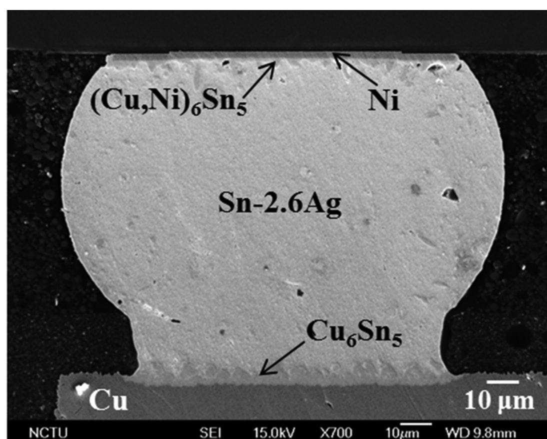

FIG. 2. Cross-sectional SEM image showing the microstructure of a as-fabricated solder bump. Ni UBM was adopted on the chip side, and Cu metallization was used on the substrate side.

TABLE I. Calibration of the real temperatures in solder joints at different hotplate temperatures.

Applied current (A)	Hotplate Temp. (°C)	Real Temp. (°C)	Joule heating (°C)
1.3	150	185	35
1.3	140	172	32
1.3	130	158	28
1.3	120	146	26
1.3	100	126	26

Table I. For example, the real temperature is 126 °C for the joint stressed by 1.3 A at an ambient temperature of 100 °C. In the following text, we will refer the real temperature as the stressing temperature.

The electromigration failure mode is attributed to void formation at the interface of the Cu UBM and solder when the joint is stressed at 126 °C. Figs. 3(a) and 3(b) show a pair of solder joints stressed by 1.3‘ A at 126 °C for 1600 h. The directions of the electron flow are labeled in the figures. The resistance increased 10 mΩ after 1600 h. The electromigration damage in both bumps cause the resistance to increase.

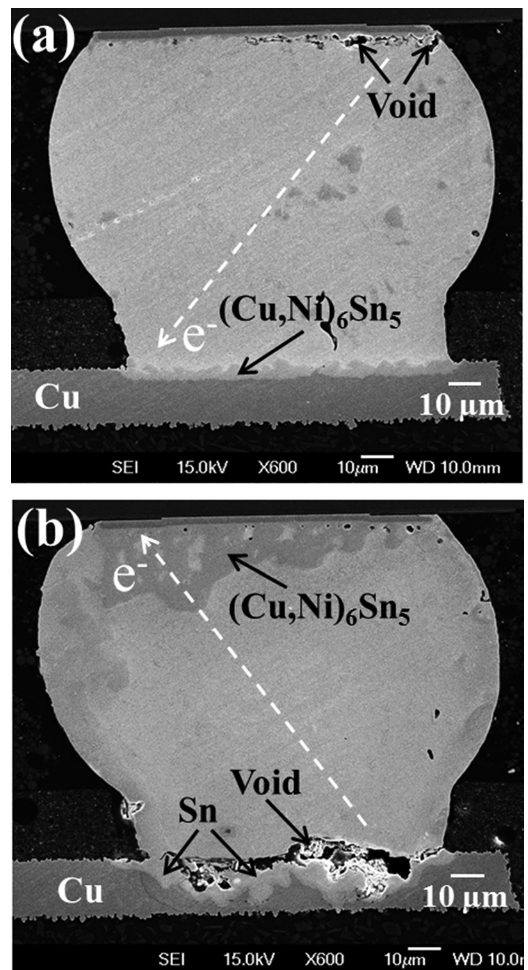

FIG. 3. The microstructure of solder joints after current stressing by 1.4×10^4 A/cm^2 at 126 °C for 1600 h. (a) With a downward electron flow. (b) With an upward electron flow. Void formation occurred at the Cu-Sn interface on the substrate side.

[This article is copyrighted as indicated in the article. Reuse of AIP content is subject to the terms at: http://scitation.aip.org/termsconditions. Downloaded to] IP: 140.113.38.11 On: Wed, 30 Apr 2014 08:48:10

For the joints with a downward electron flow, some voids formed in the upper right corner of the joint, which is current crowding region. The voids located between $(Ni,Cu)_3Sn_4$ IMCs and the solder as shown in Fig. 3(a). A layer type $(Cu,Ni)_6Sn_5$ formed on the substrate side. For the solder bump with an upward electron flow, a large amount of voids formed on the substrate side, which is the current crowding region as shown in Fig. 3(b). In fact, the voids are located in the interface of $(Cu,Ni)_6Sn_5$ IMCs and the solder. The results indicate that solder was migrated to the chip side, and vacancies accumulated at the interface. On the other hand, voids also formed in the interface of Cu metallization and solder on the substrate side for the bump with an upward electron flow.

As the stressing temperature increase to 136 °C, void formation also dominates the electromigration failure mechanism. Figures 4(a) and 4(b) show the cross-sectional SEM images for another pair of solder joints stressed at 136 °C for 1702 h. The resistance increased by 10 mΩ after the current stressing. Void formation occurred in the Ni/solder interface, as shown in Fig. 4(a). For the solder bump with an upward electron flow, serious void formation was also observed at the interface of the $(Cu,Ni)_6Sn_5$ IMCs and the solder, as presented

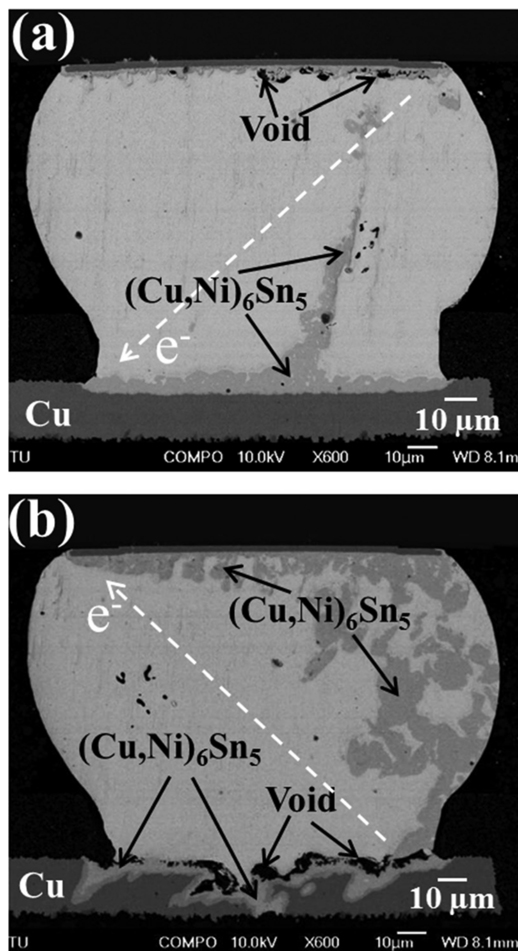

FIG. 4. The microstructure of solder joints after current stressing by 1.4×10^4 A/cm^2 at 136 °C for 1702 h. (a) With a downward electron flow. (b) With an upward electron flow. Thickening of Cu-Sn IMC took place at the Cu-Sn interface on the substrate side.

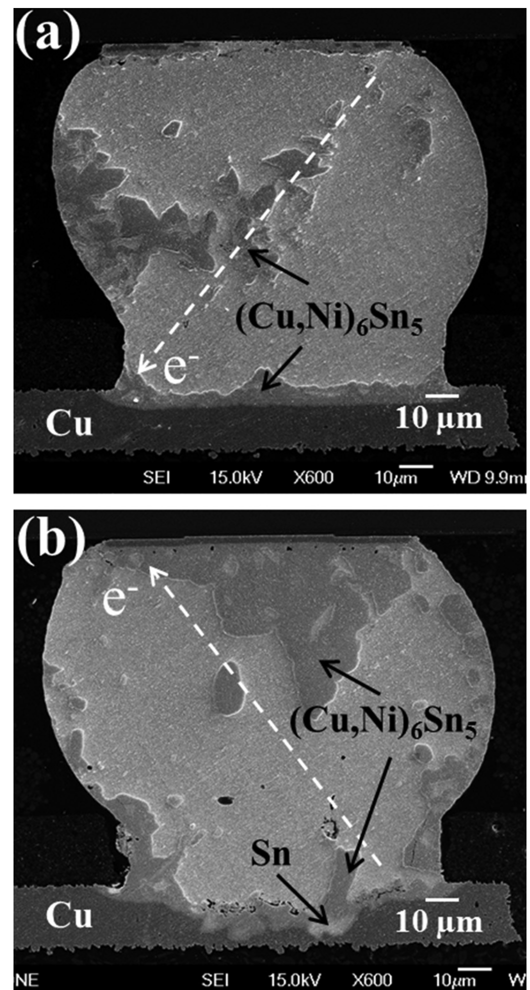

FIG. 5. The microstructure of solder joints after current stressing by 1.4×10^4 A/cm^2 at 158 °C for 260 h. (a) With a downward electron flow. (b) With an upward electron flow. Serious Cu dissolution and Cu-Sn IMC formation were observed at the Cu-Sn interface on the substrate side.

in Fig. 4(b). This microstructure change indicates that void formation dominates the failure mechanism at 136 °C.

However, the failure mode switches to Cu dissolution when the stressing temperatures increase beyond 158 °C. Figure 5(a) shows the microstructure after current stressing at 158 °C for 260 h. The Ni UBM was visibly consumed. The Ni UBM becomes discontinuous as the Ni UBM on the right-hand side completely migrated to the solder to form $(Cu,Ni)_6Sn_5$ IMCs. However, no obvious void formation was observed at the interface of the Ni UBM and the solder. The results for the Cu/solder interface, which was stressed at 158 °C, are presented in Figure 5(b). Extensive dissolution of Cu on the cathode occurred, and a significant amount of $(Cu,Ni)_6Sn_5$ IMCs accumulated on the anode/chip end. Few voids formed at the Cu/solder interface. The formation of the Cu-Sn and Ni-Sn IMCs also contributed to the resistance increase of the solder joints. The electrical resistivity of Cu, Ni, and SnAg solder is 1.7, 6.8, and 12.3 $\mu\Omega$ cm, respectively. Nevertheless, the resistivity of Cu_6Sn_5 and Ni_3Sn_4 IMCs is 17.5 and 28.5 $\mu\Omega$ cm, respectively.[36]

As the stressing temperature increased to 172 °C, the Ni UBM was almost completely consumed after 140 h. As

[This article is copyrighted as indicated in the article. Reuse of AIP content is subject to the terms at: http://scitation.aip.org/termsconditions. Downloaded to] IP: 140.113.38.11 On: Wed, 30 Apr 2014 08:48:10

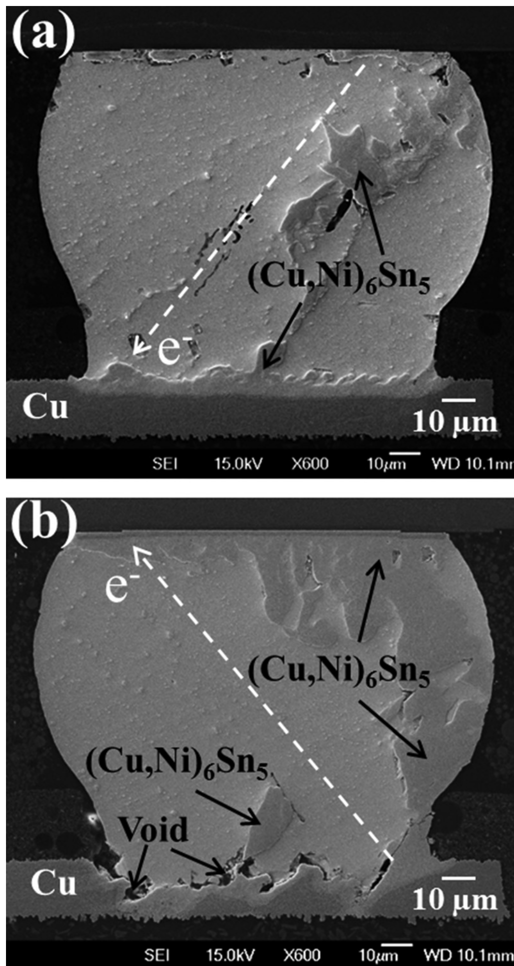

FIG. 6. Cross-sectional SEM image showing the microstructure of solder joints after current stressing by 1.4×10^4 A/cm^2 at 172 °C for 140 h. (a) With a downward electron flow. (b) With an upward electron flow. Serious Cu dissolution and Cu-Sn IMC formation were observed at the Cu-Sn interface on the substrate side. Some voids formed at the interface.

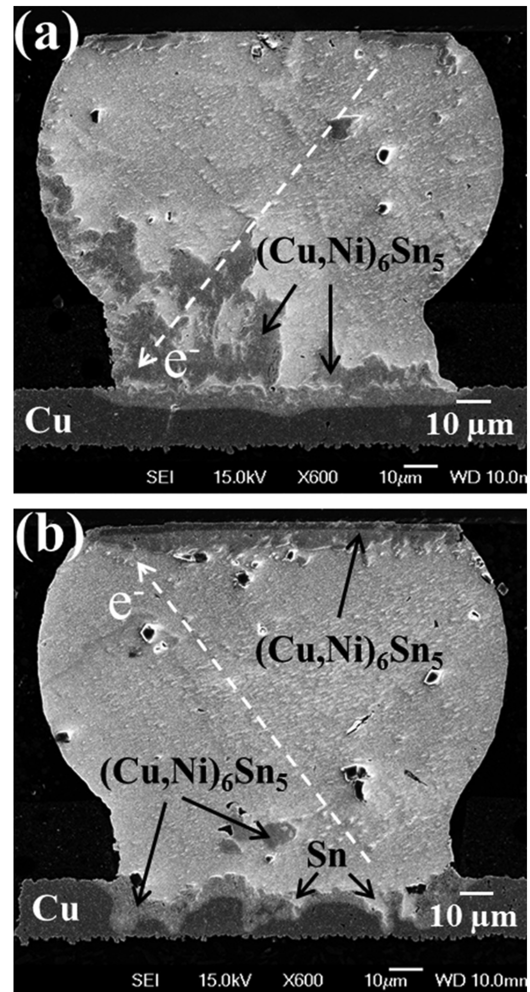

FIG. 7. Cross-sectional SEM image showing the microstructure of solder joints after current stressing by 1.4×10^4 A/cm^2 at 185 °C for 56 h. (a) With a downward electron flow. (b) With an upward electron flow. Extensive Cu dissolution and Cu-Sn IMC formation were found at the Cu-Sn interface on the substrate side. Almost no voids were observed at the interface.

shown in Figure 6(a), the Ni UBM migrated to the solder and formed significant amounts of $(Cu,Ni)_6Sn_5$ IMCs in the solder. Few voids were observed at the original Cu/solder interface. Conversely, extensive Cu dissolution and IMC formation also occurred in the Cu/solder interface, as illustrated in Figure 6(b). Although some voids formed at the Cu/solder interface, they were not significant, as demonstrated in Figure 3(b). When the temperature increased to 185 °C, rapid dissolution of the Cu and Ni UBMs occurred. Figures 7(a) and 7(b) depict the microstructures of the two bumps stressed at 185 °C for 56 h. The 2-μm Ni UBM almost completely migrated to the solder through electromigration, resulting in the formation of large amounts of $(Cu,Ni)_6Sn_5$ IMCs on the substrate side, as shown in Figure 7(a). Although large amounts of Ni atoms migrated, no discernible voids formed in the vicinity of the original Ni/solder interface on the chip side. For the electromigration in Cu metallization in Figure 7(b), significant Cu dissolution also occurred at the cathode end on the substrate. The Cu line on the substrate side exhibits a thickness of 20 μm. Although Cu was almost completely consumed at some locations, few voids were generated at the Cu/solder interface.

IV. THEORETICAL ANALYSIS OF FLUX DIVERGENCE AT THE Cu_6Sn_5/SOLDER INTERFACE

To explain the temperature-dependent failure mode, we developed a model to calculate the electromigration flux of Cu and Sn at the Cu_6Sn_5/solder interface. Fig. 8(a) includes a schematic drawing of the solder joint that was subjected to an upward electron flow. Due to electromigration, Cu atoms migrated to the Cu_6Sn_5 (η') layer and the Sn2.6Ag solder. Three distinct fluxes were assumed due to electromigration: Cu flux in the η' IMC layer, $J_{Cu\,in\,\eta'}$; Cu flux in the solder, $J_{Cu\,in\,Sn}$; and Sn flux in the solder, $J_{Sn\,in\,Sn}$. We ignore the Cu and Sn fluxes due to chemical potential. If $J_{Cu\,in\,\eta'}$ is larger than $J_{Cu\,in\,Sn}$, the thickness of the interfacial IMC increases. Conversely, if $J_{Cu\,in\,Sn}$ is larger than $J_{Cu\,in\,\eta'}$, the thickness of the interfacial IMC decreases. Considering the flux divergence at the interface between the solder and the IMC, if the net flux of Cu is larger than the Sn flux, the interfacial IMC will expand, and no voids will form at the interface. When the outgoing Sn flux at the interface is larger than the incoming Cu flux at the interface, voids form at the interface. In this section, we calculate the three fluxes by quantitatively

[This article is copyrighted as indicated in the article. Reuse of AIP content is subject to the terms at: http://scitation.aip.org/termsconditions. Downloaded to] IP: 140.113.38.11 On: Wed, 30 Apr 2014 08:48:10

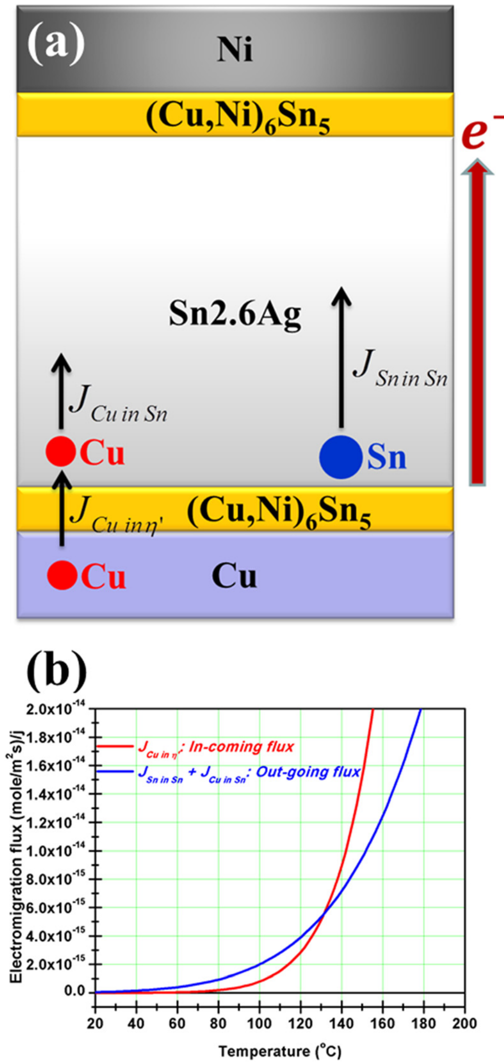

FIG. 8. (a) Schematic drawing of a solder joint subject to an upward electron flow. Three electromigration fluxes at the Cu-Sn interface were also labeled. (b) The calculated curves for the in-coming and out-going fluxes at temperature range from 20 °C to 200 °C.

incorporating available data from the literature. The electromigration flux, J_{EM}, is typically expressed as[37]

$$J_{EM} = C\frac{D}{RT}Z^{*}e\rho j, \tag{1}$$

where C is concentration, D is diffusivity, T is temperature, R is gas constant, Z^* is effective charge number, e is electron charge, ρ is resistivity, and j is current density. The Cu flux in the η' IMC layer can be expressed as follows:

$$J_{Cu\,in\,\eta'} = C_{Cu\,in\,\eta'}\frac{D_{Cu\,in\,\eta'}}{RT}Z^{*}_{Cu\,in\,\eta'}e\rho_{\eta'}j. \tag{2}$$

Because the diffusivity of Cu in $(Cu,Ni)_6Sn_5$ IMCs was not available, we used the diffusivity of Cu in η' IMC, which is expressed as follows:[38]

$$D_{Cu\,in\,\eta'} = 6.2\times10^{-8}\times\exp\left(-\frac{80500}{RT}\right)\ (\mathrm{m^2/s}). \tag{3}$$

The Z^* of Cu in the Cu_6Sn_5 IMC is 87.[39] The $\rho_{\eta'}$ is the resistivity of Cu_6Sn_5.[40] The Cu flux in solder is expressed as follows:

$$J_{Cu\,in\,Sn} = C_{Cu\,in\,Sn}\frac{D_{Cu\,in\,Sn}}{RT}Z^{*}_{Cu\,in\,Sn}e\rho_{Sn}j. \tag{4}$$

Because the Sn weights exceed 97% in the SnAg solder and the Cu diffusivity in Sn $D_{Cu\,in\,Sn}$was measured, we take $D_{Cu\,in\,Sn}$ as the diffusivity of Cu in solder,[41] which is expressed as follows:

$$D_{Cu\,in\,Sn} = 2.4\times10^{-7}\times\exp\left(-\frac{33020}{RT}\right)\ (\mathrm{m^2/s}). \tag{5}$$

The Z^* for Cu in Sn is 3.25 (Ref. 42), and the resistivity of Sn is $1.23\times10^{-7}\,\Omega\,\mathrm{m}$. The concentration of Cu in Sn, as a function of temperature, can be expressed as follows:[43,44]

$$\begin{aligned} C_{Cu\,in\,Sn} &= 0.9\times\exp\left(-\frac{37500}{RT}\right)\ (\mathrm{at\,\%}) \\ &= 5.61\times10^{6}\exp\left(-\frac{37500}{RT}\right)\ (\mathrm{mol/m^3}). \end{aligned} \tag{6}$$

In the solder near the Cu-Sn IMC, Sn will migrate toward the chip side by electron flow. The Sn flux is expressed as

$$J_{Sn} = C_{Sn}\frac{D_{Sn}}{RT}Z^{*}_{Sn}e\rho_{Sn}j, \tag{7}$$

where the Z^* of Sn is 9.6,[45] the self-diffusivity of Sn is[46]

$$D_{Sn} = 1.2\times10^{-9}\times\exp\left(-\frac{43890}{RT}\right)\ (\mathrm{m^2/s}). \tag{8}$$

Thus,

$$J_{Sn} = ej\left[1.09\times10^{-11}\times\frac{1}{T}\times\exp\left(-\frac{43890}{RT}\right)\right]. \tag{9}$$

Considering the interface between the Cu_6Sn_5 and the solder, the incoming Cu flux is $J_{Cu\,in\,\eta'}$ whereas the outgoing flux is $(J_{Cu\,in\,Sn}+J_{Sn})$. We substitute the parameters and obtain the incoming and outgoing fluxes as a function of temperature. The unit for the electromigration flux is $\mathrm{mol/m^2\,s}$, and the unit for concentration is $\mathrm{mol/m^3}$. Therefore, the density of Sn is $6.24\times10^{4}\,\mathrm{mol/m^3}$.

The Cu concentration in Cu_6Sn_5 is also dependent on temperature. We obtain the solubility limit from the Cu-Sn phase diagram[47] and solve the temperature dependence of Cu in η'. The Cu in η' can be obtained as follows:

$$C_{Cu\,in\,\eta'} = 5.50\times10^{6}\times\exp\left(-\frac{242}{RT}\right)\ (\mathrm{mol/m^3}). \tag{10}$$

With these parameters, we can plot the electromigration flux at the Cu_6Sn_5/solder interface as a function of temperature. Fig. 8(b) displays the curves for the incoming and outgoing fluxes in the temperature range of 20 °C–200 °C. The results indicate a crossover at 131 °C, below which the outgoing flux is larger than the incoming flux. Therefore, voids may form at the interface. In contrast, the incoming flux is larger than the outgoing flux, which results in the dissolution of Cu

[This article is copyrighted as indicated in the article. Reuse of AIP content is subject to the terms at: http://scitation.aip.org/termsconditions. Downloaded to] IP: 140.113.38.11 On: Wed, 30 Apr 2014 08:48:10

and extensive IMC formation, but without void formation. The theoretic calculations successfully explain the experimental results.

V. DISCUSSION

Several experimental results obtained by other researchers support the results of this study. Lin *et al*. reported extensive Cu-Sn IMC formation when the interface of Cu and Sn was stressed by 3.28×10^3 A/cm^2 at 160 °C.[48] However, when the interface was stressed by 5.3×10^3 A/cm^2 at 55 °C, numerous large voids formed at the interface.[49] Xu *et al*. performed electromigration tests under conditions of 2.0×10^4 A/cm^2 and 135 °C, in which both mechanisms were observed.[19] Therefore, temperature-dependent electromigration failure occurs in the Cu and Sn interfaces.

It is interesting that some Sn atoms migrated against electron flow and back filled the original position of the Cu metallization on the substrate side, as shown in Figs. 3(b), 5(b), and 7(b). This phenomenon may be attributed to back stress of electromigration.[50,51] The Cu and Sn were migrated to the chip side due to electromigration. Yet, the solder joints were confined by the underfill, and there were no hillocks or extrusion on the chip side to release the compressive stress on the chip side. On the other hand, tensile stress was developed on the substrate side because the deficiency of Sn and Cu atoms. Therefore, a stress gradient was built up across the solder joints, which triggered the migration of Sn to the original location of Cu metallization. In addition, chemical potential may also cause the diffusion of Sn atoms to the Cu end. Sn atoms tend to form Cu-Sn IMCs on the Cu-Sn interface to lower the free energy. As the Cu atoms were migrated away from the substrate side by the electron flow, Sn atoms may diffuse back to the Cu surface. This chemical potential force may increase as the temperature increases because the Cu-Sn reaction rate is higher at high temperatures. As shown in Figs. 5(b) and 7(b), extensive Cu dissolution took place, and most of them were migration to the chip side. Nevertheless, Sn atoms diffused against electromigration and filled the original Cu position, resulting in almost no voids formed in the substrate side.

It is noteworthy that voids may form at later stages of electromigration even at high temperatures. Especially, when the Cu is consumed completely, voids will occur because the in-coming Cu flux becomes zero.[24]

The electromigration behavior at the Ni_3Sn_4/solder interface appears similar to that at Cu_6Sn_5/solder interface. As presented in Figs. 3(a)–7(a), voids formed at the interface of $(Ni,Cu)_3Sn_4$/solder at 126 °C–185 °C. Yet, Ni dissolution becomes more significant as the temperature increases. However, the diffusion parameters Ni in $(Ni,Cu)_3Sn_4$ IMCs are currently not available. It deserves more study and analysis.

Chemical potential may also affect the Sn flux at the IMC/solder interface because Sn atoms tend to move to the Cu to form Cu-Sn IMCs. Therefore, the Sn flux due to chemical potential diffuses against electron flow for the joints with upward electron flow. In the following, we will

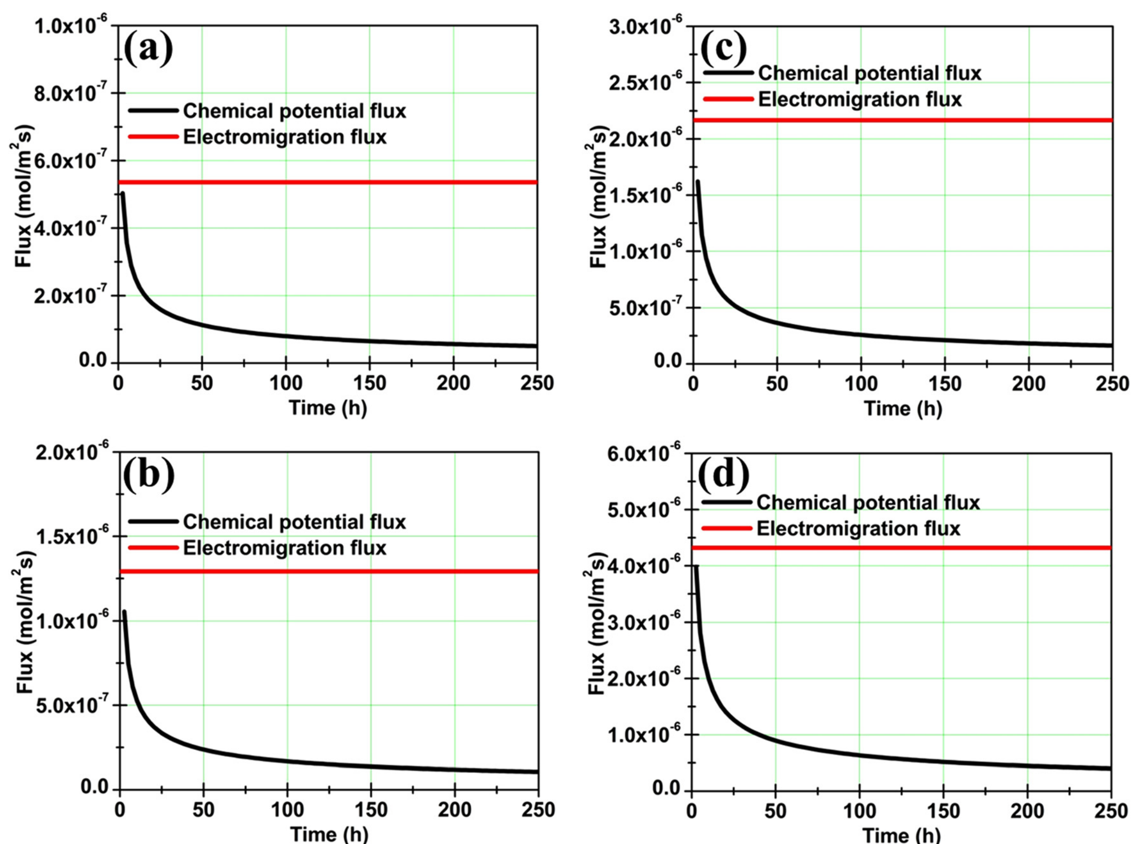

FIG. 9. The calculated Sn flux attributed to chemical potential and electromigration-induced Sn flux by 1.4×10^4 A/cm^2 at (a) 120 °C; (b) 150 °C; (c) 170 °C; and (d) 200 °C.

[This article is copyrighted as indicated in the article. Reuse of AIP content is subject to the terms at: http://scitation.aip.org/termsconditions. Downloaded to] IP: 140.113.38.11 On: Wed, 30 Apr 2014 08:48:10

calculate the Sn flux at the stressing conditions adopted in this study. We will take the IMC growth rate constants published in literature and estimate the Sn flux due to the chemical potential. The Sn flux attributed to the chemical potential is

$$J_{Sn\,in\,IMC} = \frac{k \times A \times V_{Sn} \times d_{Sn}}{V_{IMC} \times M_{Sn} \times A \times t}, \quad (11)$$

where k is IMC growth rate constant, A is area, V_{Sn} is molar volume of Sn, d_{Sn} is density of Sn, V_{IMC} is molar volume of IMC, M_{Sn} is atomic weight of Sn, and t is time. The IMC growth rate constant for Cu_6Sn_5 IMC in a Sn-Cu-Ni system is 0.2232 μm/h$^{0.5}$ at 150 °C.[52] With these parameters, we can plot the electromigration-induced Sn flux using Eq. (7) and the Sn flux due to chemical potential as a function of time. Figures 9(a) through 9(d) show the calculated results at temperature 120 °C, 150 °C, 170 °C, and 200 °C, respectively. The results indicate that the Sn flux due to chemical potential is smaller than the electromigration flux in the stressing conditions in this study. Therefore, it is reasonable to neglect the flux due to chemical potential in this work.

VI. CONCLUSIONS

In summary, we investigated the electromigration failure mechanism in solder joints with Cu UBM at temperatures ranging from 126 °C to 185 °C. Void formation at the Cu_6Sn_5/solder interface caused failure at low temperatures. However, the dissolution of Cu UBM and the formation of Cu-Sn IMC dominated the failure mechanism at high temperatures. By considering the flux divergence at the Cu_6Sn_5/solder interface, we proposed a model to calculate the electromigration flux at the interface. The results indicate that the outgoing flux is larger than the incoming flux at temperatures below 131 °C. However, the reverse trend is observed for temperatures above 131 °C. This model successfully explains the observed experimental results.

ACKNOWLEDGMENTS

The authors gratefully acknowledge the financial support of the National Science Council of the Republic of China (Grant No. NSC 99-2221-E-009-040-MY3).

[1] K. N. Tu, J. Appl. Phys. **94**, 5451 (2003).
[2] K. N. Tu, *Solder Joint Technology* (Springer, New York, 2007).
[3] K. Zeng and K. N. Tu, Mater. Sci. Eng. R. **38**, 55 (2002).
[4] J. H. Lau, *Flip Chip Technology* (McGraw-Hill, New York, 1996), p. 123.
[5] M. Abtew and G. Selvaduray, Mater. Sci. Eng., R. **27**, 95 (2000).
[6] K. N. Tu, Microelectron. Reliab. **51**, 517 (2011).
[7] J. C. Lin, W. C. Chiou, K. F. Yang, H. B. Chang, Y. C. Lin, E. B. Liao, J. P. Hung, Y. L. Lin, P. H. Tsai, Y. C. Shih, T. J. Wu, W. J. Wu, F. W. Tsai, Y. H. Huang, T. Y. Wang, C. L. Yu, C. H. Chang, M. F. Chen, S. Y. Hou, C. H. Tung, S. O. Jeng, and D. C. H. Yu, "High density 3D integration using CMOS foundry technologies for 28 nm node and beyond," in *IEEE International Electron Device Meeting* (2010), pp. 2.1.1–2.1.4.
[8] A. Yu, J. H. Lau, S. W. Ho, A. Kumar, W. Y. Hnin, D. Q. Yu, M. C. Jong, V. Kripesh, D. Pinjala, and D. L. Kwong, "Study of 15 μm pitch solder microbumps for 3D IC integration," in *Electronic Components and Technology Conference (ECTC)* (2009), pp. 6–10.
[9] C. Chen, H. M. Tong, and K. N. Tu, Annu. Rev. Mater. Sci. **40**, 531 (2010).
[10] Y. C. Chan, A. C. K. So, and J. K. L. Lai, Mater. Sci. Eng., B. **55**, 5 (1998).
[11] C. Chen, H. Y. Hsiao, Y. W. Chang, F. Y. Ouyang, and K. N. Tu, Mater. Sci. Eng. R. **73**, 85 (2012).
[12] S. Brandenburg and S. Yeh, "Electromigration studies of flip-chip solder bump solder joints," in *Proceedings of Surface Mount International Conference and Exhibition, San Jose* (1998), pp. 337–344.
[13] C. Y. Liu, C. Chen, C. N. Liao, and K. N. Tu, Appl. Phys. Lett. **75**, 58 (1999).
[14] Y. W. Chang, S. W. Liang, and C. Chen, Appl. Phys. Lett. **89**, 032103 (2006).
[15] T. L. Shao, Y. H. Chen, S. H. Chiu, and C. Chen, J. Appl. Phys. **96**, 4518 (2004).
[16] H. K. Kim and K. N. Tu, Appl. Phys. Lett. **67**, 2002 (1995).
[17] C. Y. Liu, J. T. Chen, Y. C. Chuang, K. Lin, and S. J. Wang, Appl. Phys. Lett. **90**, 112114 (2007).
[18] C. Y. Liu, L. Ke, Y. C. Chuang, and S. J. Wang, J. Appl. Phys. **100**, 083702 (2006).
[19] L. H. Xu, J. K. Han, J. J. Liang, K. N. Tu, and Y. S. Lai, Appl. Phys. Lett. **92**, 262104 (2008).
[20] B. Chao, S. H. Chae, X. F. Zhang, K. H. Lu, M. Ding, J. Im, and P. S. Ho, J. Appl. Phys. **100**, 084909 (2006).
[21] P. G. Kim, J. W. Jang, and T. Y. Lee, J. Appl. Phys. **86**, 6746 (1999).
[22] H. F. Hsu and S. W. Chen, Acta Mater. **52**, 2541 (2004).
[23] C. Schmetterer, H. Flandorfer, and H. Ipser, Acta Mater. **56**, 155 (2008).
[24] H. Y. Chen, M. F. Ku, and C. Chen, Adv. Mater. Res. **1**, 83 (2012).
[25] H. Y. Chen and C. Chen, J. Mater. Res. **26**, 983 (2011).
[26] H. Y. Chen and C. Chen, J. Mater. Res. **25**, 1847 (2010).
[27] E. C. C. Yeh, W. J. Chos, K. N. Tu, P. Elenius, and H. Balkan, Appl. Phys. Lett. **80**, 580 (2002).
[28] J. R. Huang, C. M. Tsai, Y. W. Lin, and C. R. Kao, J. Mater. Res. **23**, 250 (2008).
[29] Y. C. Hu, Y. H. Lin, C. R. Kao, and K. N. Tu, J. Mater. Res. **18**, 2544 (2003).
[30] Y. L. Lin, C. W. Chang, C. M. Tsai, C. W. Lee, and C. R. Kao, J. Electron. Mater. **35**, 1010 (2006).
[31] J. H. Ke, T. L. Yang, Y. S. Lai, and C. R. Kao, Acta Mater. **59**, 2462 (2011).
[32] T. L. Shao, T. S. Chen, Y. M. Huang, and C. Chen, J. Mater. Res. **19**, 3654 (2004).
[33] S. J. Wang and C. Y. Liu, Scr. Mater. **55**, 347 (2006).
[34] S. H. Chiu, T. L. Shao, and C. Chen, Appl. Phys. Lett. **88**, 022110 (2006).
[35] H. Y. Hsiao, S. W. Liang, M. F. Ku, C. Chen, and D. J. Yao, J. Appl. Phys. **104**, 033708 (2008).
[36] C. Chen and S. W. Liang, J. Mater. Sci.: Mater. Electron. **18**, 259 (2007).
[37] H. B. Hungtington and A. R. Grone, J. Phys. Chem. Solids **20**, 76 (1961).
[38] A. Paul, C. Ghosh, and W. J. Boettinger, Metall. Mater. Trans. A **42**, 952 (2011).
[39] S. Ou and K. N. Tu, "A study of electromigration in Sn3.5Ag and Sn3.8Ag0.7Cu solder lines," in *Electronic Components and Technology Conference (ECTC)* (2005), pp. 1445–1450.
[40] H. P. R. Frederikse, R. J. Fields, and A. Feldman, J. Appl. Phys. **72**, 2879 (1992).
[41] B. F. Dyson, T. R. Anthony, and D. Turnbull, J. Appl. Phys. **38**, 3408 (1967).
[42] M. Y. Hsieh and H. B. Huntington, J. Phys. Chem. Solids **39**, 867 (1978).
[43] J. H. Shim, C. S. Oh, B. J. Lee, and D. N. Lee, Zeitschrift für Metallkunde **87**, 205 (1996), available at http://cat.inist.fr/?aModele=afficheN&cpsidt=3010941.
[44] K. W. Moon, W. J. Boettinger, U. R. Kattner, F. S. Biancaniello, and C. A. Handwerker, J. Electron. Mater. **29**, 1122 (2000).
[45] P. H. Sun and M. Ohring, J. Appl. Phys. **47**, 478 (1976).
[46] W. Seith and T. Heumann, *Diffusion of Metals: Exchange Reactions* (Springer, Berlin, 1962), pp. 65, 68.
[47] N. Saunders and A. P. Miodownik, *ASM Handbook: Alloy Phase Diagrams*, edited by H. Baker (ASM International, Materials Park, Ohio/Second Publishing, Inc., 1991), Vol. 3, p. 2.178.
[48] C. T. Lin, Y. C. Chuang, S. J. Wang, and C. Y. Liu, Appl. Phys. Lett. **89**, 101906 (2006).
[49] H. W. Tseng, C. T. Lu, Y. H. Hsiao, P. L. Liao, Y. C. Chuang, T. Y. Chung, and C. Y. Liu, Microelectron. Reliab. **50**, 1159 (2010).
[50] I. A. Blech and C. Herring, Appl. Phys. Lett. **29**, 131 (1976).
[51] F. Y. Ouyang, K. Chen, and K. N. Tu, Appl. Phys. Lett. **91**, 231919 (2007).
[52] J. W. Yoon, Y. H. Lee, D. G. Kim, H. B. Kang, S. J. Suh, C. W. Yang, C. B. Lee, J. M. Jung, C. S. Yoo, and S. B. Jung, J. Alloys Compd. **381**, 151 (2004).

[This article is copyrighted as indicated in the article. Reuse of AIP content is subject to the terms at: http://scitation.aip.org/termsconditions. Downloaded to] IP: 140.113.38.11 On: Wed, 30 Apr 2014 08:48:10